

Supporting Information

Optical and Electrical Properties of Efficiency Enhanced Polymer Solar Cells with Au Nanoparticles in PEDOT-PSS Layer

Dixon D.S. Fung¹, Linfang Qiao^{1,2}, Wallace C.H. Choy¹, Chuandao Wang¹, Wei E.I. Sha¹, Fengxian
Xie¹, Sailing He^{1,2}*

¹ Department of Electrical and Electronic Engineering, University of Hong Kong, Pokfulam Road, Hong
Kong, China.

² Centre for Optical and Electromagnetic Research, State Key Laboratory of Modern Optical
Instrumentations, Zhejiang University, Hangzhou 310058, China.

Supplementary A

In order to understand the detail physics of plasmonic effects of Au NPs in PEDOT:PSS on the light absorption of the P3HT:PCBM active layer, we build an efficiency model to rigorously solve Maxwell's equations. We adopt the fast algorithm of volume integral equation - Fast Fourier transform (VIE-FFT) to solve Maxwell's equations. Details of the model are described as below.

1. Volume Integral Equation Method

The scattered electric field generated by the volumetric polarization current \mathbf{J} can be written as

$$\mathbf{E}^s(\mathbf{r}) = -j_0\omega\mu_0 \int_v \overline{\mathbf{G}}(\mathbf{r}, \mathbf{r}') \cdot \mathbf{J}(\mathbf{r}') d\mathbf{r}' \quad (1)$$

where ω is the angular frequency, and $\overline{\mathbf{G}}(\mathbf{r}, \mathbf{r}')$ is the dyadic Green's function given by

$$\overline{\mathbf{G}}(\mathbf{r}, \mathbf{r}') = \left(\overline{\mathbf{I}} + \frac{\nabla\nabla}{k_0^2} \right) g(\mathbf{r}, \mathbf{r}'), \quad g(\mathbf{r}, \mathbf{r}') = \frac{\exp(-jk_0|\mathbf{r}-\mathbf{r}'|)}{4\pi|\mathbf{r}-\mathbf{r}'|} \quad (2)$$

where k_0 is the wavenumber of free space. For the non-magnetic optical materials ($\mu_r = 1$), the volume integral equation (VIE) is of form

$$\mathbf{E}^i(\mathbf{r}) = \frac{\mathbf{J}(\mathbf{r})}{j_0\omega(\varepsilon(\mathbf{r}) - \varepsilon_0)} - \mathbf{E}^s(\mathbf{r}) \quad (3)$$

where $\varepsilon(\mathbf{r})$ is the position-dependent permittivity of the inhomogeneous materials, and $\mathbf{E}^i(\mathbf{r})$ is the incident electric field.

Considering the Cartesian coordinate system, we use the short notation (u_1, u_2, u_3) substituting for (x, y, z) , then we have

$$\begin{bmatrix} E_1^s \\ E_2^s \\ E_3^s \end{bmatrix} = \begin{bmatrix} L_{11} & L_{12} & L_{13} \\ L_{21} & L_{22} & L_{23} \\ L_{31} & L_{32} & L_{33} \end{bmatrix} \begin{bmatrix} J_1 \\ J_2 \\ J_3 \end{bmatrix} \quad (4)$$

where

$$L_{ij} = \begin{cases} L_{ii}^c + L_{ii}^q, & i = j \\ L_{ij}^q, & i \neq j \end{cases} \quad (5)$$

$$L_{ii}^c J_i = -j_0 \omega \mu_0 \int_V g(\mathbf{r}, \mathbf{r}') J_i(\mathbf{r}') d\mathbf{r}' \quad (6)$$

$$L_{ij}^q J_j = \frac{-j_0}{\omega \varepsilon_0} \frac{\partial}{\partial u_i} \int_V g(\mathbf{r}, \mathbf{r}') \frac{\partial J_j(\mathbf{r}')}{\partial u_j} d\mathbf{r}' \quad (7)$$

Using the rooftop basis functions to expand the unknown currents, we have

$$\mathbf{J}(\mathbf{r}) = \sum_{i=1}^3 \mathbf{u}_i \sum_{k,m,n} J_i^D(k, m, n) T_{k,m,n}^i \quad (8)$$

where $T_{k,m,n}^1$, $T_{k,m,n}^2$, and $T_{k,m,n}^3$ are the volumetric rooftop functions given by

$$\begin{aligned} T_{k,m,n}^1 &= \Lambda_k(u_1) \Pi_m(u_2) \Pi_n(u_3) \\ T_{k,m,n}^2 &= \Pi_k(u_1) \Lambda_m(u_2) \Pi_n(u_3) \\ T_{k,m,n}^3 &= \Pi_k(u_1) \Pi_m(u_2) \Lambda_n(u_3) \end{aligned} \quad (9)$$

The functions $\Lambda_k(u_1)$ and $\Pi_m(u_2)$ are defined by

$$\begin{aligned} \Lambda_k(u_1) &= \begin{cases} 1 - \frac{|u_1 - k\Delta u_1|}{\Delta u_1}, & |u_1 - k\Delta u_1| \leq \Delta u_1 \\ 0, & \text{else} \end{cases} \\ \Pi_m(u_2) &= \begin{cases} 1, & \left| u_2 - \left(m - \frac{1}{2} \right) \Delta u_2 \right| < \frac{\Delta u_2}{2} \\ 0, & \text{else} \end{cases} \end{aligned} \quad (10)$$

The cuboid cells are employed to discretize the structure to be modeled. Here, Δu_1 and Δu_2 are the grid sizes of each small cuboid along x and y directions, respectively. Other functions in (9) can be defined as the same way.

As a result, the discretized form for the operator L_{ii}^c in (6) can be written as

$$L_{ii}^{D,c} J_i^D = -j_0 \omega \mu_0 g^D \otimes J_i^D \quad (11)$$

where \otimes denotes the discrete convolution

$$g^D \otimes J_i^D = \sum_{k,m,n} g^D(k-k', m-m', n-n') J_i^D(k', m', n') \quad (12)$$

and

$$g^D(k, m, n) = \int_0^{\Delta u_1} \int_0^{\Delta u_2} \int_0^{\Delta u_3} g(u_{1,k} - u'_1, u_{2,m} - u'_2, u_{3,n} - u'_3) du_1 du_2 du_3 \quad (13)$$

Likewise, the operator $L_{12}^{D,q}$ in (7) can be discretized as

$$\begin{aligned} L_{12}^{D,q} J_2^D &= \frac{-j_0}{\omega \varepsilon_0 \Delta u_1 \Delta u_2} \left[g^D(k+1, m, n) - g^D(k, m, n) \right] \\ &\otimes \left[J_2^D(k, m, n) - J_2^D(k, m-1, n) \right] \\ &= \frac{-j_0}{\omega \varepsilon_0 \Delta u_1 \Delta u_2} \left\{ \left[g^D(k+1, m, n) - g^D(k, m, n) \right] \right. \\ &\quad \left. - \left[g^D(k+1, m-1, n) - g^D(k, m-1, n) \right] \right\} \otimes J_2^D(k, m, n) \end{aligned} \quad (14)$$

where the finite-difference method is used for the smooth approximation of the dyadic Green's function.

The computations of the discrete convolutions can be performed efficiently by means of cyclic convolutions and fast Fourier transform (FFT), which is similar to the discrete dipole approximation (DDA) method.

2. The Biconjugate Gradient Stabilized Algorithm

The resulting VIE matrix equation can be expressed as

$$Ax = b$$

The procedure of the biconjugate gradient stabilized (BI-CGSTAB) algorithm is given as follows:

Give an initial guess x_0 , we have

$$r_0 = b - Ax_0, \hat{r}_0 = r_0$$

$$\rho_0 = \alpha = \omega_0 = 1$$

$$v_0 = p_0 = 0$$

Iterate for $i = 1, 2, \dots, n$

$$\begin{aligned}\rho_i &= \langle \hat{r}_0, r_{i-1} \rangle \\ \beta &= (\rho_i / \rho_{i-1}) (\alpha / \omega_{i-1}) \\ p_i &= r_{i-1} + \beta (p_{i-1} - \omega_{i-1} v_{i-1}) \\ v_i &= A p_i \\ \alpha &= \rho_i / \langle \hat{r}_0, v_i \rangle \\ s &= r_{i-1} - \alpha v_i \\ t &= A s \\ \omega_i &= \langle t, s \rangle / \langle t, t \rangle \\ x_i &= x_{i-1} + \alpha p_i + \omega_i s \\ r_i &= s - \omega_i t\end{aligned}$$

Terminate when

$$\frac{\|r_i\|_2}{\|b\|_2} < \eta$$

where η is the tolerance that specifies the desired accuracy of solution.

3. Optical Absorption of active material

The optical absorption of the active layer, which determines the electron-hole pair generation rate, can be calculated by

$$A = \int n_r n_i \omega \varepsilon_0 |\mathbf{E}(\mathbf{r})|^2 dV, \quad \mathbf{E}(\mathbf{r}) = \frac{\mathbf{J}(\mathbf{r})}{j\omega(\varepsilon(\mathbf{r}) - 1)}$$

where \mathbf{J} is the volumetric polarization current obtained, $\varepsilon = (n_r - j_0 n_k)^2$, and n_r and n_i are the real and imaginary parts of the complex refractive index of the active material.

Supplementary Figures

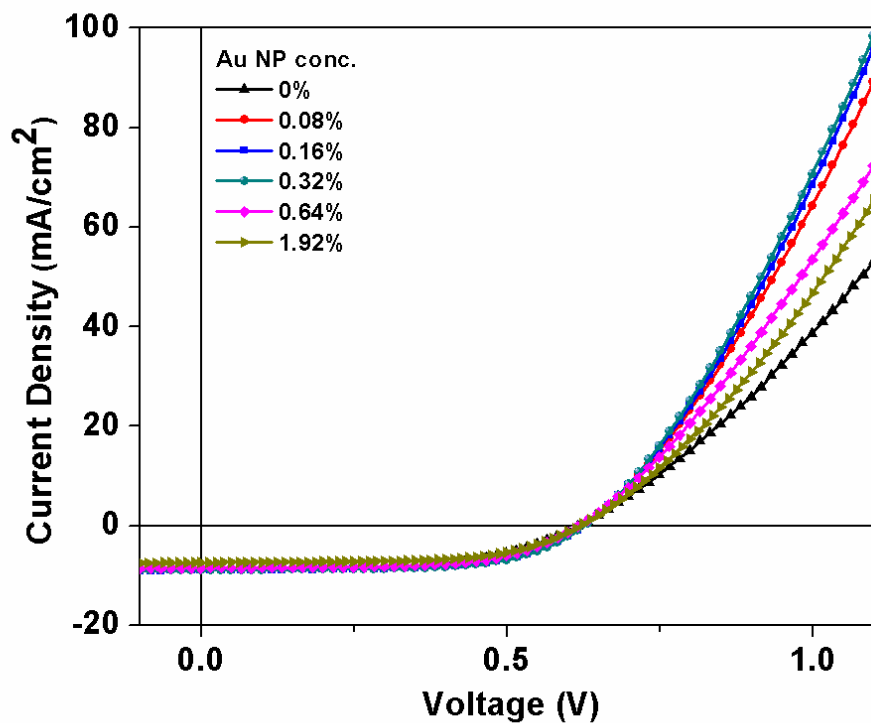


Fig. S1. *J-V* characteristics of solar cells with structures ITO/PEDOT:PSS(with PEG-capped Au NPs)/P3HT:PCBM/LiF(1nm)/Al(100nm), incorporated with different NP concentrations under AM 1.5G illumination at 100 mW/cm². Comparing to Fig. 1 in the manuscript, the x-axis is extended to show the increase in forward bias injection current.

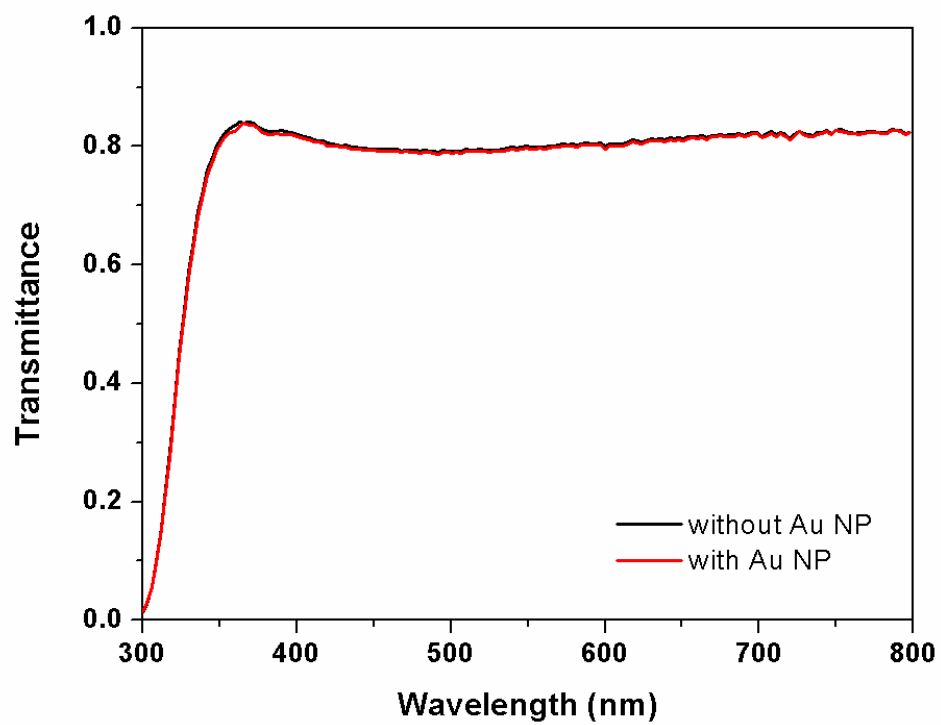


Fig. S2. Transmittance of Glass/ITO/PEDOT:PSS (with or without NPs).

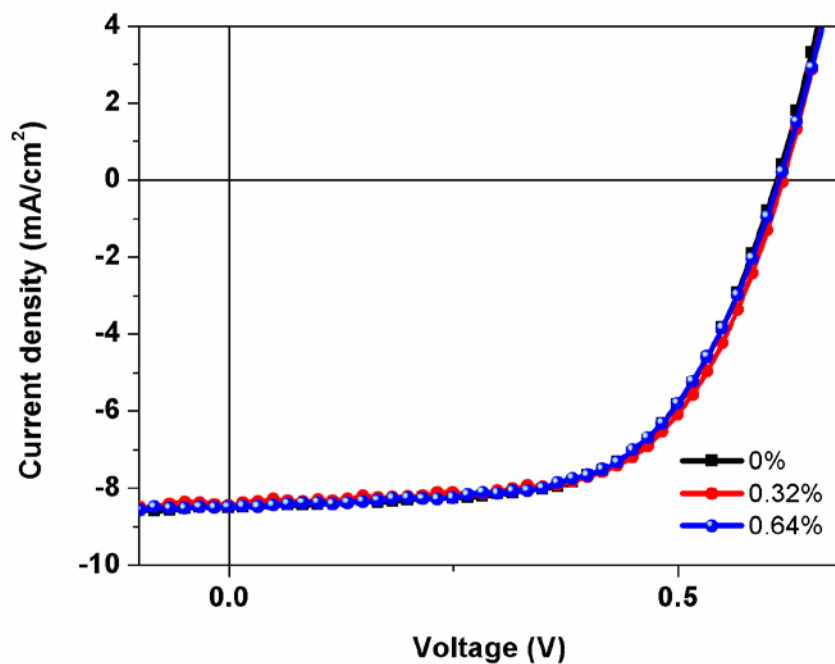


Figure S3. Comparisons of JV characteristics of devices with structure ITO/PEDOT:PSS: AuNPs/PEDOT:PSS/P3HT:PCBM/LiF/Al, for different Au NPs concentrations.

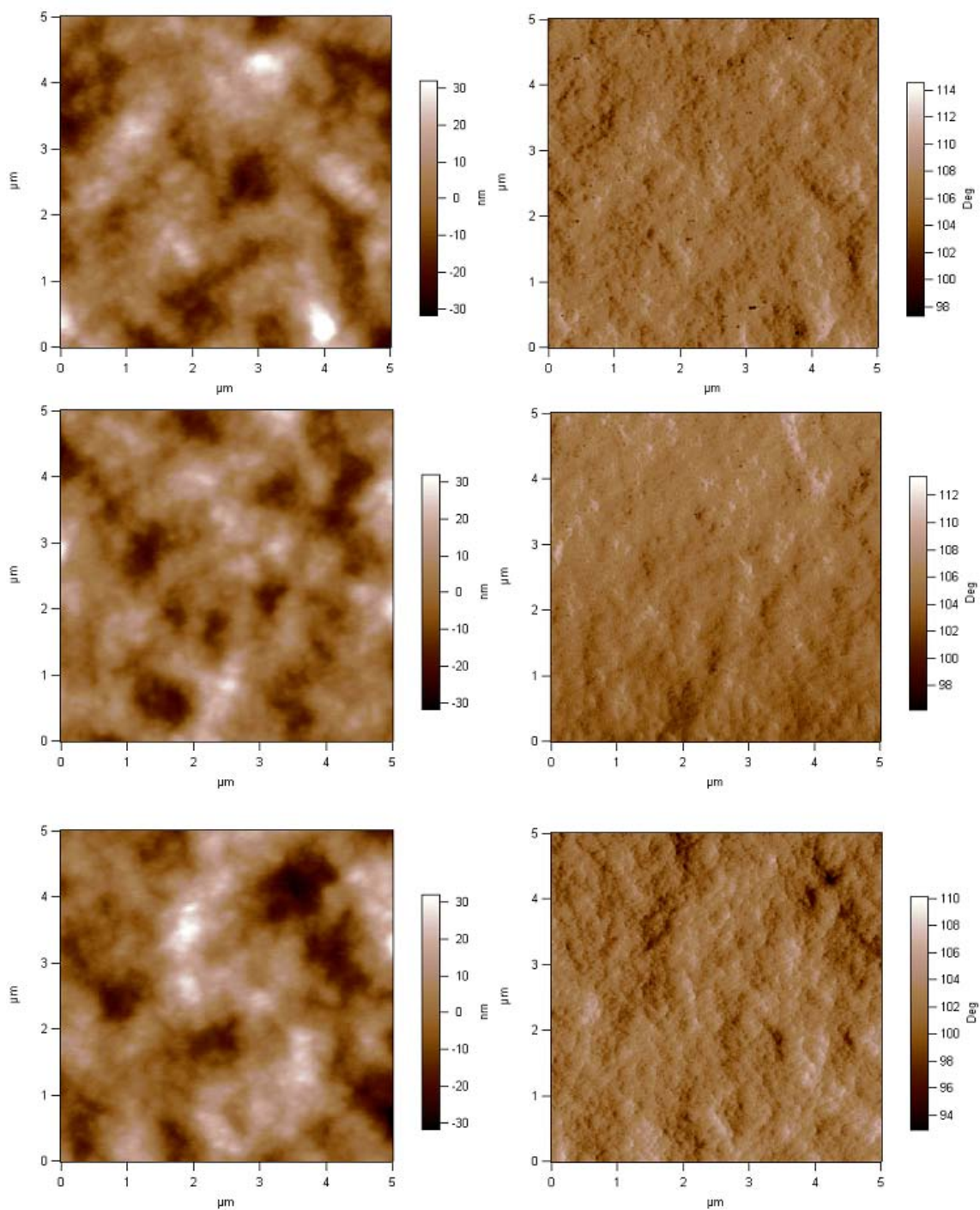


Figure S4. AFM height (left) and phase (right) images of P3HT:PCBM layer. Concentrations of Au NPs in PEDOT:PSS are 0% (top), 0.32%(middle), 1.92% (bottom).